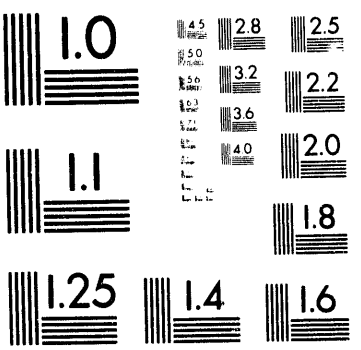
1.0
1.1
1.25
1.4
1.6
1.8
2.0
2.2
2.5
2.8
3.2
3.6
4.0
4.5
5.0
5.6
6.3
7.1

1 of 1

LBL-34367
DA-302

The Energy Performance of Prototype Holographic Glazings

K. Papamichael, L. Beltrán, R. Furler, E.S. Lee, S. Selkowitz, M. Rubin

Energy and Environment Division
Lawrence Berkeley Laboratory
University of California
Berkeley, California 94720

February 1993

This work was supported by the Assistant Secretary for Conservation and Renewable Energy, Office of Building Technologies, Building Systems and Materials Division of the U.S. Department of Energy under Contract No. DE-AC03-76SF00098.

February 1993

The Energy Performance of Prototype Holographic Glazings

K. Papamichael, L. Beltrán, R. Furler, E.S. Lee, S. Selkowitz, M. Rubin

Building Technologies Program
Energy and Environment Division
Lawrence Berkeley Laboratory
Berkeley, CA 94720

1.0 Executive Summary

We report on the simulation of the energy performance of prototype holographic glazings in commercial office buildings in a California climate. These prototype glazings, installed above conventional side windows, are designed to diffract the transmitted solar radiation and reflect it off the ceiling, providing adequate daylight illumination for typical office tasks up to 30 ft (9.14 m) from the window.

Past studies on the daylight performance of previous versions of these holographic glazings indicate that they can reduce electric lighting loads over a deeper perimeter area than clear glass for selected sun positions. However, no data have been available to estimate potential energy savings over the course of an entire year, under more realistic combined sun and sky conditions and for different window orientations. Moreover, these previous studies have not accounted for the cooling loads from solar heat gain associated with the use of daylight, which must be considered along with daylighting savings to estimate the overall efficiency improvement.

In this study, we experimentally determined a comprehensive set of solar-optical properties and characterized the contribution of the prototype holographic glazings to workplane illuminance in a scale model of a typical office space. We then used the scale model measurements to simulate the energy performance of the holographic glazings over the course of an entire year for four window orientations (North, East, South and West) for the inland Los Angeles climate, using the DOE-2.1D building energy analysis computer program.

The results of our experimental analyses indicate that these prototype holographic glazings diffract only a small fraction of the incident light.

The average diffraction efficiency, defined as the fraction of the incident visible radiation diffracted towards the ceiling, was estimated at 16%-20% for the most effective angle of incident radiation. As a result, the daylight performance of these holographic glazings is very similar to clear glass. The same is true with the solar heat gain performance, since the holographic diffractive structures have only a minimal effect on the near infrared part of the solar spectrum and were applied on single clear glass.

Previous versions of these holographic diffractive structures show higher diffraction efficiency, in the range of 35% - 40%. However, these previous versions produce an undesired "rainbow" effect. The new versions show a significant improvement with respect to producing "white" light. However, this improvement in light quality has apparently been achieved at a cost of reduced diffraction efficiency.

When compared to low-E glazing with shading control, which is considered to be the current common practice for improved energy efficiency, holographic glazings reduced total annual electric energy requirements by 3% on the North orientation but increased them by 26%, 41% and 32% on the East, South and West orientations, respectively. Holographic glazings reduced annual electric lighting requirements by 11%, 10%, 3% and 7% on the North, East, South and West orientations, respectively. They also reduced cooling loads due to solar heat by 7% on the North orientation, but increased them by 50%, 71% and 58% on the East, South and West orientations, respectively. Finally, holographic glazings increased peak electricity demand by 6%, 30%, 36% and 32%, on North, East, South and West, orientations, respectively.

Since the holographic diffractive structures may be applied to thermally better glazings than single-pane clear glass, we modeled various hypothetical glazings assuming the daylight performance of the holographic glazings and the thermal performance of double and double low-E glazings. While performance improved, it was still not as good as that of double low-E glazing with shading control. We also considered shading with single-pane holographic glazing, which provided better performance with respect to reducing cooling loads but worse with respect to daylighting (electric lighting savings), being overall less energy-efficient than low-E glazing with shading control.

The results of this study indicate that these prototype holographic glazings will not save energy in commercial office buildings. Their performance is very similar to that of clear glass, which, through side windows, cannot efficiently illuminate more than a 15 ft - 20 ft (4.57 m - 6.09 m) depth of a building's perimeter, because the cooling penalties due to solar heat gain are greater than the electric lighting savings due to daylighting.

It should be possible to improve the energy performance of holographic glazings, by redesigning their light control function and

by integrating them with solar heat gain control technologies into more sophisticated fenestration systems. However, if this technology is to produce marketable energy-efficient products, additional research and development is required to integrate the holographic structures into complete window / curtain-wall designs, considering the overall building performance with respect to energy, cost and comfort.

2.0 Introduction

When combined with appropriate electric lighting dimming controls, the use of daylight for task illumination can significantly reduce energy requirements in commercial buildings. While skylights can effectively illuminate any part of one-story buildings, conventional side windows can illuminate only a 15 ft - 20 ft (4.57 m - 6.09 m) depth of the building perimeter. Even so, the overall efficacy of daylight is limited, because side windows produce uneven distributions of daylight. Achieving adequate illumination at distances further away from the window results in excessive illumination near the window, which increases cooling loads from the associated solar heat gain. As a result, the use of larger apertures and/or higher transmittance glazings, to introduce daylight deeper than 15 ft - 20 ft (4.57 m - 6.09 m), may prove ineffective with respect to saving energy, because the cooling load penalties may exceed the electric lighting savings.

The need for more uniform distributions of daylight admitted through side windows has stimulated significant research and development efforts in new fenestration designs and glazing technologies. Many of these approaches rely on the common strategy of redirecting daylight and reflecting it off the ceiling towards the back of the room. This should provide daylight illumination at distances up to 30 ft (9.14 m) from the window without excessive daylight and solar heat gain near the window.

Holographic glazings use a coating of microscopic diffractive structure to redirect light. One such coating is being developed by the Advanced Environmental Research Group (AERG), which was founded in 1984 to conduct research and development on the use of Holographic Diffractive Structures (HDS) in windows.

2.1 Background

The first AERG HDS samples were analyzed in 1989, using outdoor measurements in a scale model that represented a 20 ft (6.09 m) wide by 30 ft (9.14 m) deep by 10 ft (3.05 m) high space with HDS glazing covering the top 4 ft (1.22 m) of the window wall [Bryan 1990]. The analysis showed that, when compared to clear glass, HDS introduce more daylight at a distance of 27.5 ft (8.38 m) from the window wall, for high sun altitudes (60° to 70°) at a plane normal to the window. However, the HDS performance decreases as the sun azimuth from the normal to the window increases, and the HDS introduce less daylight than clear glass under overcast skies. Moreover, these initial HDS

samples produce a rainbow effect, since different parts of the visible spectrum are diffracted at different angles.

Since the 1989 study, AERG developed a new generation of sample gratings, which use five-stripe bands of HDS designed to mix the outgoing radiation and eliminate the rainbow effect. We will refer to these new samples as BHDS (B stands for "banded"). Analyses performed by AERG, using indoor measurements in a model similar to the 1989 study, indicate that, when compared to clear glass, BHDS introduce more daylight at a distance of 27.5 ft (8.38 m) from the window wall, for sun altitudes ranging from 30° to 70° at a plane normal to the window [AERG 1992].

The above studies indicate that the use of the BHDS can save lighting energy by reducing electric lighting loads over a deeper perimeter area than clear glass, for a limited range of sun positions. However, no data have been available to estimate total energy savings (heating, cooling and lighting) for the course of a whole year and for different window orientations, taking into account daylighting for all sun and sky conditions, and the cooling loads from solar heat gain associated with the use of daylight.

2.2 Objective

The agencies sponsoring this research have as their objective the development and commercialization of efficient building technologies. To realize the large market impact sought by the sponsoring agencies, new glazing technologies must exceed the performance of existing energy efficient glazings.

The objective of this study was to determine the energy performance of the prototype BHDS glazings in a typical office building in a California climate and compare it with that of existing energy efficient windows.

The focus of this study was to provide a sufficiently detailed characterization of the solar-optical properties of the holographic coatings so that a comprehensive annual energy analysis could be performed.

3.0 Methodology

As explained in the previous section, the effectiveness of daylight utilization for energy savings depends on the balance of electric lighting savings due to daylighting and cooling load penalties due to solar heat gain. The performance of a fenestration system is dynamic and depends on the context of its application, which is characterized by parameters such as building type, window orientation and climate.

Considering the above, we decided to determine the energy performance of the BHDS sample gratings assuming office building activities and schedules, for four orientations (North, East, South and

West) and compare it with the energy performance of double pane low-E glazing with shading control, which represents current common practice with respect to energy-efficient glazings. We also decided to consider a California climate, because it offers the opportunity for proper consideration of the trade-off between electric lighting savings due to daylighting and cooling load penalties due to solar heat gain.

We selected a 20 ft (6.09 m) by 30 ft (9.14 m) space with 10 ft (3.05 m) height, with BHDS covering the whole width of the window wall from a 6 ft (1.83 m) to 10 ft (3.05 m) height, and low-E glazing covering the whole width of the window wall from a 3 ft (0.91 m) to 6 ft (1.83 m) height from the floor plane (Figure 1). We then compared the performance to the "base case" of an identical space with double low-E glazing with shading control, covering the whole width of the window wall from 3 ft (0.91 m) to 10 ft (3.05 m) height (Figure 2). The modeled space was considered as part of a 16,000 square feet office building, with 20 ft (6.09 m) by 30 ft (9.14 m) perimeter office spaces surrounding an 80 ft (24.36 m) by 80 ft (24.36 m) core zone.

AERG provided us with one 4 inch by 5 inch BHDS sample, two 2 inch by 5 inch BHDS samples, two 2 inch by 2.5 inch BHDS samples, and one 4 inch by 5 inch HDS sample, for measurements required for simulation analyses. These BHDS sample gratings were designed to provide optimal results for the modeled configuration facing South.

In order to determine the energy performance of the BHDS samples, we had to determine their daylight and thermal performance. The optical complexity of the AERG sample gratings prevented us from using conventional, computer-based simulation methods. Thus, we employed a new method, which is based on the use of scale models to experimentally determine directional illuminance coefficients, which are then used with analytical, computer-based routines. This method allows us to simulate the daylight performance of fenestration systems and spaces of arbitrary complexity under any exterior conditions, and use the results with the DOE-2.1D energy analysis computer program [BESG 1984a, 1984b] that provides an hour-by-hour simulation of the operation of a building for the course of a whole year.

4.0 Smoke Chamber Photographs

Initially, we took photographs of a laser beam transmitted through the BHDS, to visualize the magnitude and direction of the transmitted radiation. One BHDS sample was placed inside a smoke chamber and a low-power red laser beam was directed at it at various incident angles and captured on film.

Visual inspection of these photographs suggest that only a small fraction of the light incident on the BHDS is redirected, while most of it is transmitted specularly, that is as through clear glass (Figures 3 and 4). Since the size of the laser beam was small and could not cover all five-stripes of the BHDS bands, we did not draw any conclusions and

decided to proceed with the scale model measurements and compare the daylight performance of the BHDS with that of clear glass.

5.0 Scale Model Photometric Analysis

After the completion of the smoke chamber photographs, AERG provided us with an improved 4 inch by 5 inch BHDS sample, referred herein as BHDS-2. Since AERG expressed a concern that the BHDS samples might have been damaged due to exposure to light and smoke, we decided to take measurements for both samples, as well as clear glass, and compare the results.

We constructed a half-inch-to-a-foot to scale model of the typical office space described in Section 3.0 (Methodology), with interior reflectance values of 0.76 for the ceiling, 0.44 for the walls and 0.21 for the floor. Using our scanning radiometer [Papamichael 1987] (Figures 5 and 6), we took measurements of workplane illuminance at 6 distances from the window wall (Figure 7) for 121 incoming directions of radiation, covering the whole hemisphere seen by the window (Figure 8). Since the BHDS-2 sample could not be used to cover the entire 2 inch by 10 inch aperture that corresponded to the holographic glazing, we decided to make two sets of comparisons, totaling 5 sets of measurements. First we made a three-way comparison among clear glass, BHDS, and BHDS-2, considering a 2 inch by 4 inch aperture (Figure 9). Then, we made a second set of measurements for a two-way comparison between clear glass and BHDS for the whole 2 inch by 10 inch aperture (Figure 10).

The results of these measurements indicate that BHDS and BHDS-2 were very similar, confirming that the smoke tests had not damaged the original sample (Figures 11, 12 and 13). When compared to clear glass, BHDS introduce more light at the back of the room for a large number of incoming directions. However, although the percent differences appear to be large (Figure 14), the actual values are small in terms of desired light levels and large for the directions that clear glass introduces more light (Figures 14, 15 and 16). The similarity of the results from BHDS when compared with clear glass are consistent with the laser beam photographs which suggest that only a small fraction of the transmitted radiation through the BHDS is redirected.

In addition to the above mentioned indoor measurements, we took several outdoor measurements to ensure that the spectral output of the light source used for the indoor measurements was appropriate. During these outdoor tests we took photographs of the model's interior for several sun positions, to document the color separation of the transmitted radiation and the luminance distribution of the interior surfaces. We also took some additional outdoor scale model photographs using the HDS sample to compare the color separation and the color mixing effectiveness of the BHDS. The photographs of the HDS show an intense rainbow effect (Figure 17), in contrast to the

BHDS which is much more effective in mixing the outgoing radiation to reduce the rainbow effect (Figure 18).

We also compared the results of our outdoor measurements with those from the 1989 study [Bryan 1990]. While we are in general agreement with respect to percent differences, there are significant disagreements with respect to actual illuminance values. The 1989 analysis used the HDS samples, rather than the BHDS coating design. However, even the clear glass measurements are in significant disagreement. The 1989 study reports up to 70 fc (752.5 lux) at a distance of 27.5 ft (8.38 m) from the window wall with clear glass. With higher outdoor illumination levels we measured 21 fc (225.75 lux) for clear glass and 24 fc (258 lux) without any glass. To better understand this discrepancy, we performed a set of additional outdoor measurements varying the ground reflectance in front of the scale model. This variation of the ground reflectance resulted in a large variation in indoor workplane illuminance from 11 fc (115 lux) with low ground reflectance (brown surface) to 56 fc (605 lux) with high ground reflectance (white surface). Since the outdoor test models are tilted to obtain the correct solar incident angle, the effect of varying ground reflectance can be large, particularly at the back of the room. A possible reason for the higher illuminance values of the 1989 study may be the use of a high ground reflectance.

6.0 Daylight Analysis

Prior to conducting an annual energy analysis, we performed a more detailed daylight analysis for the San Francisco, CA, climate, considering four orientations (North, East, South and West) for twelve instances in a year (9:00 AM, 12:00 Noon and 3:00 PM, for March 21, June 21, September 21 and December 21). The daylight analysis was performed for both: the 4 ft (1.22 m) by 8 ft (2.44 m) aperture comparing clear glass, BHDS and BHDS-2, and the 4 ft (1.22 m) x 20 ft (6.1 m) aperture comparing clear glass and BHDS.

Daylight values for the sun, sky, and ground components were determined using the experimentally determined directional workplane illuminance coefficients of the photometric analysis. Values for the sun component were determined through interpolation on the measured coefficients. Values for the sky and ground components were determined through integration of the measured coefficients over the luminance distribution of the sky and the ground. We assumed the CIE clear and overcast sky luminance distributions [CIE 1970, 1973] and 0.2 uniform ground reflectance.

The results of the daylight analysis indicate that the BHDS and BHDS-2 introduce more light from the sun than clear glass at the back of the room when the sun is at high altitudes in front of the window, such as during the summer noon hours for a South-facing window (Figure 19). However, when the sun is at low altitudes, such as during the winter noon hours for a South-facing window the HDS and BHDS introduce

less sunlight than clear glass (Figure 20). Clear glass always introduces more light from the sky than the holographic glazings throughout the space (Figure 21). The differences in light contribution from the sky is even more profound for the 4 ft (1.22 m) by 20 ft (6.1 m) aperture. In many cases the extra light from the sky introduced through clear glass balances out the extra light from the sun introduced by the holographic glazings, even for the South-facing window at summer noon (Figure 22), when the BHDS and BHDS-2 show their best performance for small apertures. Moreover, the BHDS and BHDS-2 always introduce high daylight levels at the front of the room, which is expected to offset some of the electric lighting savings, by producing excessive cooling loads.

7.0 Radiometric Analysis

Using a goniospectrometer and our scanning radiometer, we measured the bi-directional transmittance and reflectance of the BHDS for various incoming directions, for both the visible and the total solar spectra. Measurements were taken in steps of one degree (1°) with respect to the outgoing angles, for six incoming directions of radiation (0°, 15°, 30°, 45°, 60° and 75° incident angles). The diffracted component of the transmitted radiation was then calculated through summation, used to approximate integration over the outgoing range of interest:

$$T_d = \int_{\vartheta=-28°}^{90°} \frac{T(\vartheta)}{\Delta\vartheta} \cdot d\vartheta \approx \sum_{\vartheta=-28°}^{90°} \frac{T(\vartheta)}{\Delta\vartheta} \cdot 1°$$

where $T(\vartheta)$ is the transmittance value at outgoing direction specified by ϑ, and $\Delta\vartheta$ is the angular response of the detector.

The results indicate that the BHDS redirect only a small fraction of the visible spectrum towards the ceiling, while the major part of the incident radiation is transmitted specularly, as for ordinary glass (Figures 23 and 24). These results are consistent with the laser beam photographs as well as the results of the scale model photometric analyses.

We also measured the visible spectrum bi-directional transmittance of the HDS for comparison purposes. The results of these measurements indicate that the HDS diffract significantly more light towards the ceiling than the BHDS (Figures 25 and 26). It appears that using the five stripe coating design (BHDS) to reduce the rainbow effect of the HDS, reduced the effectiveness of redirecting the light towards the ceiling. AERG believes that the diffraction efficiency of the BHDS could be brought up to that of the HDS, through better construction and elimination of the spaces between the stripes.

With respect to the total solar spectrum, the results indicate that the BHDS do not redirect any of the non-visible part of the solar radiation.

From the total spectrum transmittance (Figure 27) and reflectance (Figure 28) measurements we determined the shading coefficient of the BHDS for various incident angles (Figure 29), using the computer program WINDOW 3.1 [W&D 1989]. Due to the similarity of the thermal performance of the BHDS with clear glass, we modeled their solar heat gain performance following the DOE-2 algorithms.

8.0 Energy Analysis

Using the DOE-2.1D energy analysis computer program [BESG 1984a, 1984b], we modeled the typical office building discussed in the methodological section in the inland Los Angeles climate. We assumed the Title 24 recommended 1.5 W/ft^2 (16.1 W/m^2) installed lighting power density with continuous dimming controls for a desired workplane illuminance of 50 fc (537.5 lux). Daylighting levels were calculated for two reference points at 2.5 ft (0.76 m) workplane height from the floor and at depths of 12.5 ft (3.81 m) and 27.5 ft (8.38 m), controlling two independent electric lighting zones covering 42% and 58% of the floor area, respectively.

We considered two fenestration designs: one representing the "base case" with double low-E glazing of 0.33 Btu/hr/ft^2/°F (1.82 W/m^2/°C) U-value, 0.61 visible transmittance and 0.41 shading coefficient, and one for the application of BHDS above a low-E "view" window (Figures 1 and 2). The low-E glazing was modeled with the use of a diffuse shading device, which was deployed when the transmitted solar radiation exceeded 30 Btu/hr/ft^2 (94.5 W/m^2) or when the glare index exceeded a value of 20. When the shading device was deployed, the shading coefficient was reduced by 40% and the visible transmittance by 65%.

The luminous / thermal performance of the low-E glazing and the associated shade control was simulated using the internal algorithms of the DOE-2.1 energy analysis program. The simulation of the BHDS performance was performed through the development of a custom function called during the execution of the DOE-2 algorithms for every hour of a whole year. This function determined the performance of the BHDS aperture through interpolation among daylight factors derived from analytical routines, which were based on the experimental data from the scale model measurements. Daylight factors were determined for a large number of sun positions on a regular grid of 15° for solar azimuth and altitude. This technique which integrates data from scale model measurements with hour-by-hour simulation algorithms is the only technique currently available to account for all of the energy-related interactions of complex glazings over the course of an entire year.

We compared the base case low-E window (case A) to the holographic coatings as supplied (case B) and to three other hypothetical versions of the holographic glazings (cases C, D, E) which improved control of solar heat gains. These additional comparisons provide useful insights

into the energy controls that would be desired in a holographic window system.

We first considered the actual BHDS sample properties, that is 1.07 U-value (single pane glass) and 0.88 shading coefficient (case B). When compared to a standard low-E window (case A), the results indicate that with respect to total electric energy requirements the BHDS are better than the base case for the North orientation by 3% and worse for the East, South and West orientations by 26%, 41% and 32%, respectively (Table 1). With respect to peak electricity demand, the BHDS are worse than the base case for all orientations by 6%, 30%, 36% and 32%, for North, East, South and West, respectively (Table 2).

For all orientations the BHDS have lower electric lighting energy use than the moderate transmittance (0.61) low-E glazing (Table 3). However, the cooling penalties due to solar heat gain introduced through the BHDS (Table 4) exceed the electric lighting savings, resulting in worse overall performance (Table 1). The better performance of the BHDS for the North orientation occurs because the daylight savings exceed the smaller solar heat gain loads.

Since the thermal performance of the BHDS as supplied was the main reason for the low performance, we considered a hypothetical BHDS window (case C) with a U-value of 0.33 (double pane glass) and a much lower shading coefficient of 0.63, assuming the same daylight performance as in case B. The results are better with respect to case B but still worse than case A for all orientations (North, East, South and West) by 0.1%, 14%, 28% and 18% with respect to total electric energy requirements (Table 1), and by 4%, 15%, 23% and 14% with respect to peak electricity demand, respectively (Table 2).

Since cooling load was still a major problem, we considered a new hypothetical window (case D)with an even lower shading coefficient (0.41, equal to the low-E case), while still maintaining the original daylight properties as in case B. This reduction of the shading coefficient by 35% from case C brought the cooling loads down, near those (but still higher) of case A. The results with respect to case A for total electric energy requirements are only marginally better for North and East orientations, by 3% and 0.5%, respectively, and worse for South and West orientations, by 5% and 2%, respectively (Table 1). With respect to peak electricity demand, they are marginally better for North orientation by 0.1%, and worse for all other orientations (East, South and West) by 3%, 4% and 2%, respectively (Table 2).

Case D shows that the penalties due to increased solar heat gain through the BHDS are not only because of the higher shading coefficient but because of the lack of any solar control (shading) for direct sunlight. However, actively controlled shading for the BHDS aperture might defeat its purpose of utilizing sunlight to illuminate the back of the room. To explore this effect, we modified case B to include dynamic control of sunlight through the holographic window, modeling a shading device that reduced the magnitude of the

transmitted radiation by 65%, without affecting the distribution of the transmitted radiation (case E). In this final analysis we considered a shading schedule for the BHDS that was triggered only by solar heat gain consideration. The results of this analysis indicate that, when compared to low-E glass, the BHDS perform worse on all orientations (North, East, South and West) with respect to total electric energy requirements by 6%, 11%, 16% and 15%, respectively (Table 1). The BHDS also perform worse with respect to peak demand for all orientations by 7%, 8%, 10% and 11%, respectively Table 2). While the shading control reduced the cooling loads considerably (Table 4), it significantly reduced the daylighting benefits as well (Table 3).

9.0 Conclusions and Recommendations

The results of our analyses indicate that the current AERG banded holographic diffractive structures (BHDS) will not save significant electric energy or reduce peak electricity demand compared to conventional energy-efficient window systems in California office buildings. The BHDS redirect only a small part of the transmitted radiation (approximately 16% on the average), the rest being specularly transmitted, as through clear glass. The BHDS thus introduce high levels of daylight at the front of the room, where there is already more than enough light from the conventional "view" window.

Compared to a lower transmittance (0.61) low-E "base case" window, the BHDS reduce annual electric lighting requirements by up to 11% on the North orientation. However, they increase annual cooling loads by up to 71% on the South orientation. The luminous and thermal performance of the BHDS is not significantly better than that of clear glass, which cannot efficiently illuminate more than 15 ft - 20 ft (4.57 m - 6.09 m) of a building's perimeter through side windows, since the solar heat gain penalties due to solar heat gain exceed the electric lighting savings due to daylighting.

The BHDS produce significantly better "white" light than the non-banded HDS, however at an apparent penalty in diffraction efficiency. The high specular component of the transmitted radiation and the angular response at low sun angles which redirects light to the ceiling at the front of the room, both reduce the overall effectiveness of the glazing. Much better control of the solar heat gain will also be required to provide significant annual energy savings.

The holographic glazings tested in this study do not show significant savings in annual energy use or peak demand. While much technical progress has been made in their development over the past decade, there are still significant hurdles which must be overcome before these prototypes can become a viable, marketable product. We group these research and development needs into three areas, which are not mutually exclusive:

1. *Overall Building Performance* — Windows have an impact on many performance parameters, such as heating, cooling, lighting, peak demand, comfort, etc. An energy-efficient window whose objective is to reduce total energy use and peak demand must satisfy these often contradictory requirements. Development of a marketable holographic window can only be successful if refinements in the optical properties of the coatings are driven by a detailed understanding of performance criteria as a function of building type, orientation, latitude, climate, and time. *These performance criteria with respect to holographic windows do not currently exist.*

2. *Windows/Curtain 'Wall' Design* — Glazing systems perform within the larger context of the window, as well as the building's interior. Parameters such as window width and height, ceiling height, interior surface reflections, etc., may greatly affect the performance of holographic glazings. While window components, such as low-E coatings, gas fills, and anti reflective coatings, can be added to a holographic glazing to help control thermal gains and losses, they will increase cost and may reduce desirable properties in other performance areas. *The integration of a holographic coating into a window and integration of the window into the curtain wall are largely unexplored issues at this time.*

3. *Holographic coating design* - Monochromatic laser measurements made by AERG on non-banded samples show 40% - 50% diffraction efficiency. White light measurements made by LBL show 35% - 40% for the sample and only 16% - 20% for the banded one, for the best possible incoming directions of radiation. If the banded holographic coatings are to be developed and marketed as energy-efficient devices, their white-light diffraction efficiency must be substantially improved, over a wide range of incoming directions of radiation. Diffraction efficiency criteria may be developed for specific building applications using computer simulations. *However, such criteria are no currently available.*

The challenge to provide an energy-efficient glazing requires the design and production of a coating, or array of coatings, that have good efficiency, proper directional control over an appropriate range of input conditions, and good spectral control to provide a pleasing interior lighting quality. This challenge has not yet been met.

10.0 Acknowledgments

This work was supported by the Assistant Secretary for Conservation and Renewable Energy, Office of Building Technologies, Building Systems and Materials Division of the U.S. Department of Energy under Contract No. DE-AC03-76SF00098.

The prototype holographic diffractive structures were provided by Advanced Environmental Research Group (AERG) with support from California Energy Commission (CEC). We appreciate the useful

comments and guidance provided by **D. Navarro** and **G. Simons** from CEC.

We also thank **J. Klems** for providing access to the scanning radiometer, **J. Warner** for taking the radiometric measurements, **D. DiBartolomeo** for automating the data acquisition procedures, and **P. Fritz** and **A. Jackaway** for constructing the scale models.

11.0 References

[AERG 1992] Advanced Energy Research Group. "Holographic Test Samples." Memorandum from AERG to LBL, 2/21/92.

[Bryan 1990] Bryan, H.; King, E. "An Evaluation of a Holographic Diffractive Glazing Material for Improved Utilization of Sunlight in Buildings." Proceedings of the 15th National Passive Solar Conference, Austin TX, March 19-22, 1990, ASES, Solar 90, pp. 181-187.

[CIE 1970] CIE. "Daylight: International recommendation for the calculation of natural light." In Technical Committee E-3.2 (Ed.), Paris, France: Commission Internationale de l'Eclairage, 1970.

[CIE 1973] CIE. "Standardization of luminance distribution of clear skies." In Technical Committee 4.2 (Ed.), Paris, France: Commission Internationale de l'Eclairage, 1973.

[BESG 1984a] Building Energy Simulation Group. "Overview of the Building Energy Analysis Program." No. LBL-19735, UC-95d. Lawrence Berkeley Laboratory, Berkeley, CA, 1984.

[BESG 1984b] Building Energy Simulation Group. "DOE-2 Supplement: Version 2.1." No. LBL-8706, Rev. 4, Suppl. Lawrence Berkeley Laboratory, Berkeley, CA, 1984.

[Papamichael 1987] Papamichael, K.M.; Klems, J.H.; Selkowitz, S.E. "A Large Scanning Radiometer for Characterizing Fenestration Systems." Proceedings of the Workshop on Optical Property Measurement Techniques, Commission of the European Communities Joint Research Center, Ispra, Italy, October 27-29, 1987.

[W&D 1988] Windows and Daylighting Group. "WINDOW 3.1: A PC Program for Analyzing Window Thermal Performance (Program Description and Tutorial)" No. LBL-25686. Lawrence Berkeley Laboratory, Berkeley, CA, 1988.

Table 1. Total Electric Energy Requirements in kWh/ft^2/yr.

	North	East	South	West
3´-10´ Low-E + Shading Tv=0.61, SC=0.41, U-value=0.33, Shading Schedule	5.29	5.740	5.81	5.74
6´-10´ BHDS Tv=function*, SC=0.883, U-value=1.07, No Shading **3´-6´: Low-E+Shading**	5.14 (-2.89%)	7.22 (+25.72%)	8.19 (+41 01%)	7.55 (+31.60%)
6´-10´ Imaginary BHDS Tv=function*, SC=0.63, U-value=0.33, No Shading **3´-6´: Low-E+Shading**	5.30 (+0.08%)	6.54 (+13.92%)	7.46 (+28.41%)	6.79 (+18.25%)
6´-10´ Imaginary BHDS Tv=function*, SC=0.41, U-value=0.33, No Shading **3´-6´: Low-E+Shading**	5.12 (-3.28%)	5.72 (-0.42%)	6.12 (+5.38%)	5.86 (+2.07%)
6´-10´: Imaginary BHDS Tv=function*, SC=0.883, U-value=1.07, Shading **3´-6´: Low-E+Shading**	5.63 (+6.46%)	6.40 (+11.38%)	6.71 (+15.55%)	6.62 (+15.25%)

Table 2. Peak Electricity Demand in W/ft^2.

	North	East	South	West
3´-10´ Low-E + Shading Tv=0.61, SC=0.41, U-value=0.33, Shading Schedule	3.68	4.26	4.17	4.31
6´-10´ BHDS Tv=function*, SC=0.883, U-value=1.07, No Shading **3´-6´: Low-E+Shading**	3.96 (+6.02)	5.55 (+30.35%)	5.65 (+35.64%)	5.60 (+30.12%)
6´-10´ Imaginary BHDS Tv=function*, SC=0.63, U-value=0.33, No Shading **3´-6´: Low-E+Shading**	3.82 (+3.63%)	4.88 (+14.69%)	5.12 (+22.78%)	4.89 (+13.65%)
6´-10´ Imaginary BHDS Tv=function*, SC=0.41, U-value=0.33, No Shading **3´-6´: Low-E+Shading**	3.68 (-0.08%)	4.38 (+2.78%)	4.33 (+3.82%)	4.40 (+2.13%)
6´-10´: Imaginary BHDS Tv=function*, SC=0.883, U-value=1.07, Shading **3´-6´: Low-E+Shading**	3.94 (+6.94%)	4.62 (+8.52%)	4.57 (+9.76%)	4.76 (+10.63%)

* The term "function" refers to the special DOE-2 function used to determine the daylight workplane illuminance based on the scale model measurements and the particular sky luminance distribution for each daylight hour and window orientation.

Table 3. Electric Lighting Requirements in kWh/ft^2/yr.

	North	East	South	West
3´-10´ Low-E + Shading Tv=0.61, SC=0.41, U-value=0.33, Shading Schedule	1.46	1.47	1.32	1.37
6´-10´ BHDS Tv=function*, SC=0.883, U-value=1.07, No Shading **3´-6´: Low-E+Shading**	1.30 (-10.74%)	1.32 (-10.19%)	1.29 (-2.65%)	1.27 (-7.04%)
6´-10´ Imaginary BHDS Tv=function*, SC=0.63, U-value=0.33, No Shading **3´-6´: Low-E+Shading**	1.30 (-10.74%)	1.32 (-10.19%)	1.29 (-2.65%)	1.27 (-7.04%)
6´-10´ Imaginary BHDS Tv=function*, SC=0.41, U-value=0.33, No Shading **3´-6´: Low-E+Shading**	1.30 (-10.74%)	1.32 (-10.19%)	1.29 (-2.65%)	1.27 (-7.04%)
6´-10´: Imaginary BHDS Tv=function*, SC=0.883, U-value=1.07, **Shading** **3´-6´: Low-E+Shading**	1.73 (+18.28%)	1.71 (+16.31%)	1.57 (+18.72%)	1.64 (+19.58%)

Table 4. Cooling Requirements in kWh/ft^2/yr.

	North	East	South	West
3´-10´ Low-E + Shading Tv=0.61, SC=0.41, U-value=0.33, Shading Schedule	2.02	2.52	2.73	2.61
6´-10´ BHDS Tv=function*, SC=0.883, U-value=1.07, No Shading **3´-6´: Low-E+Shading**	1.88 (-6.98%)	3.77 (+49.74%)	4.66 (+70.81%)	4.11 (+57.61%)
6´-10´ Imaginary BHDS Tv=function*, SC=0.63, U-value=0.33, No Shading **3´-6´: Low-E+Shading**	2.21 (+9.48%)	3.36 (+33.49%)	4.21 (+54.28%)	3.65 (+39.68%)
6´-10´ Imaginary BHDS Tv=function*, SC=0.41, U-value=0.33, No Shading **3´-6´: Low-E+Shading**	1.99 (-1.15%)	2.65 (+5.20%)	3.06 (+12.25%)	2.83 (+8.24%)
6´-10´: Imaginary BHDS Tv=function*, SC=0.883, U-value=1.07, **Shading** **3´-6´: Low-E+Shading**	1.96 (-2.60%)	2.81 (+11.55%)	3.22 (+17.83%)	3.03 (+16.14%)

* The term "function" refers to the special DOE-2 function used to determine the daylight workplane illuminance based on the scale model measurements and the particular sky luminance distribution for each daylight hour and window orientation.

Figure 1.

The window configuration considered as the **BHDS application.**

holographic glazing

double low-E glazing

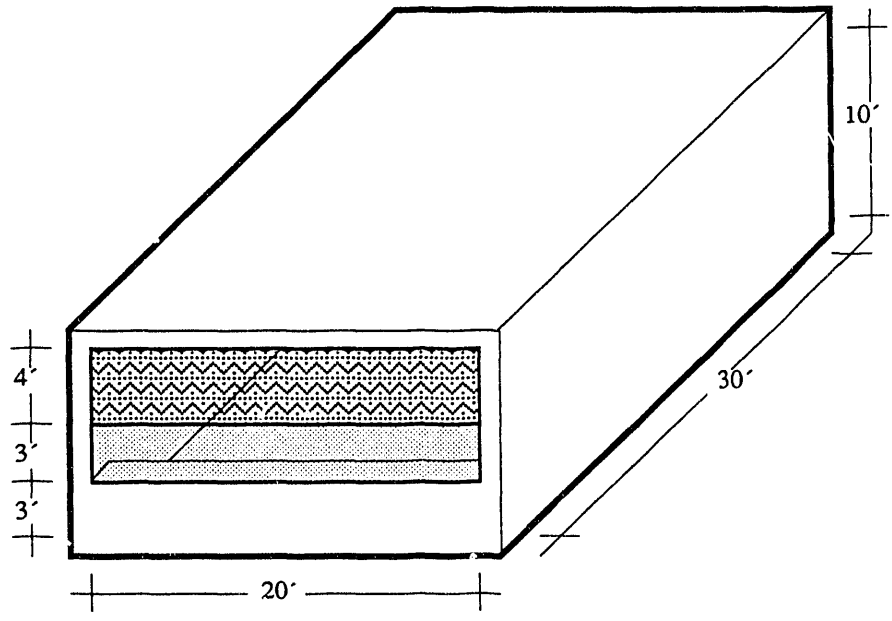

Figure 2.

The window configuration considered as the **"base case."**

double low-E glazing

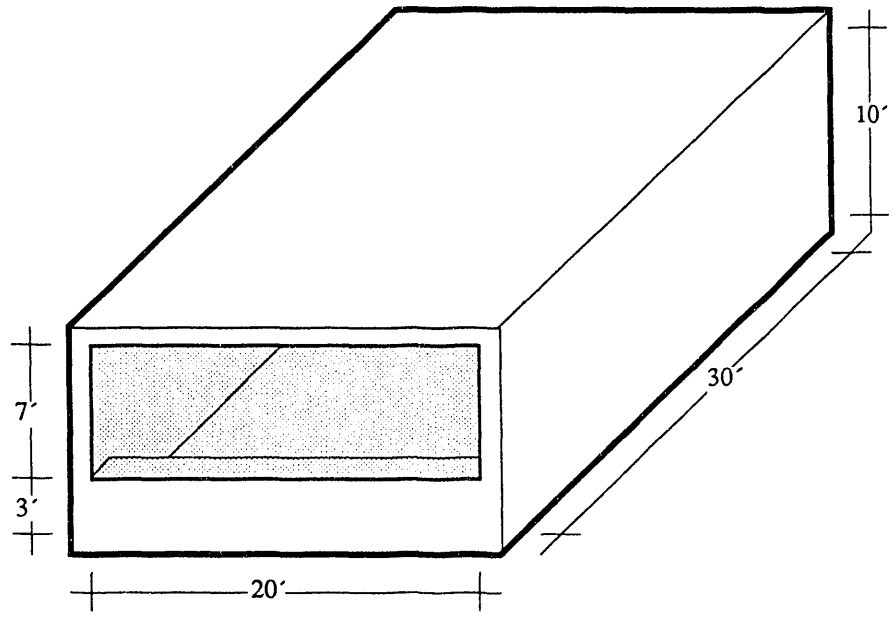

Figure 3.

Photograph of a laser beam transmitted through BHDS for **15°** incident angle.

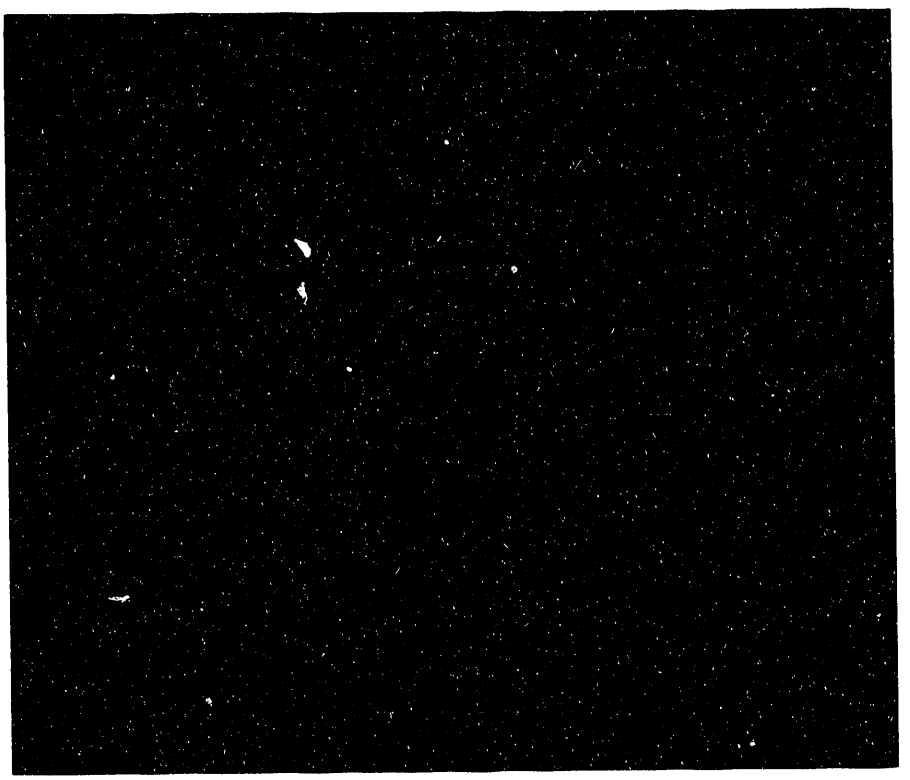

Figure 4.

Photograph of a laser beam transmitted through BHDS for **60°** incident angle.

Figure 5.

Front view of the scanning radiometer with the scale model used for the directional workplane illuminance measurements.

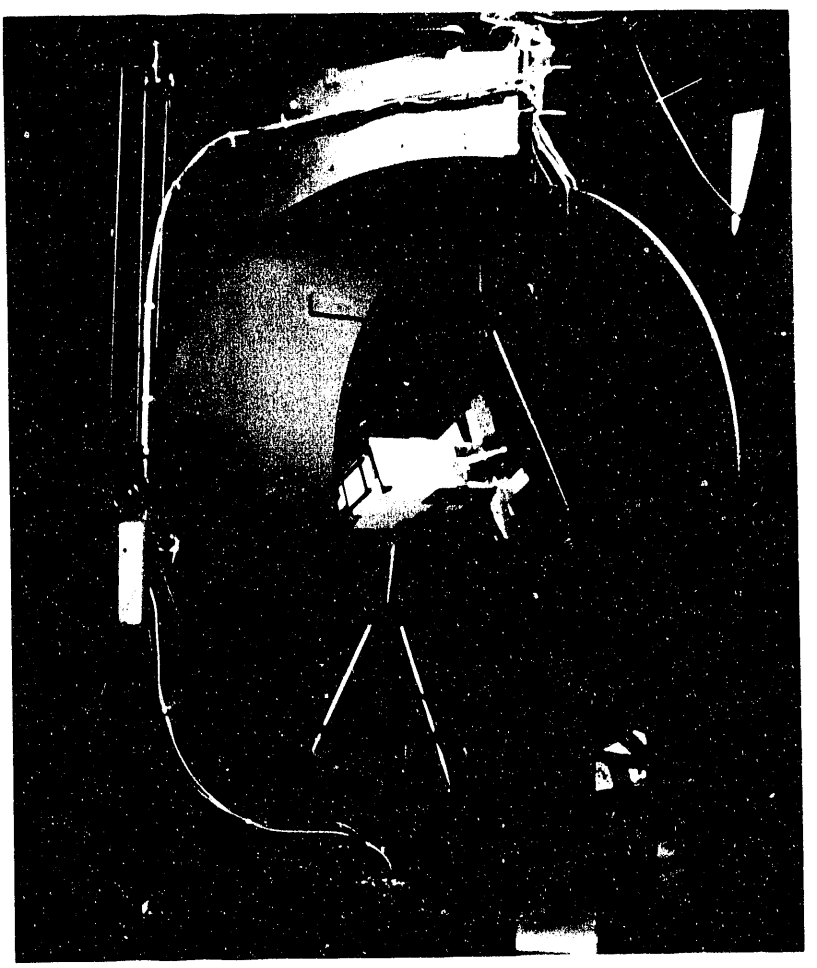

Figure 6.

Rear view of the scanning radiometer with the scale model used for the directional workplane illuminance measurements.

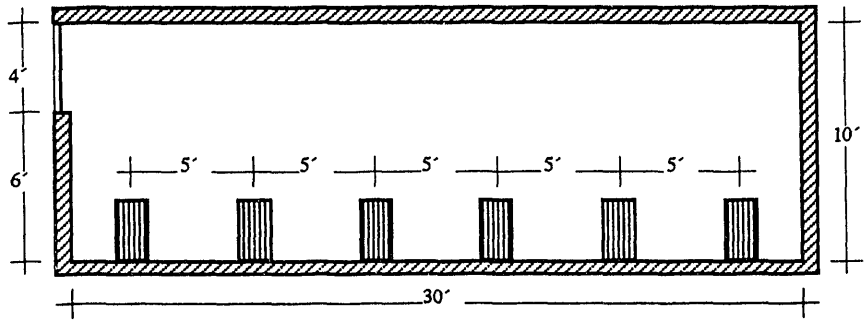

Figure 7.

The workplane reference points considered for the directional workplane illuminance measurements.

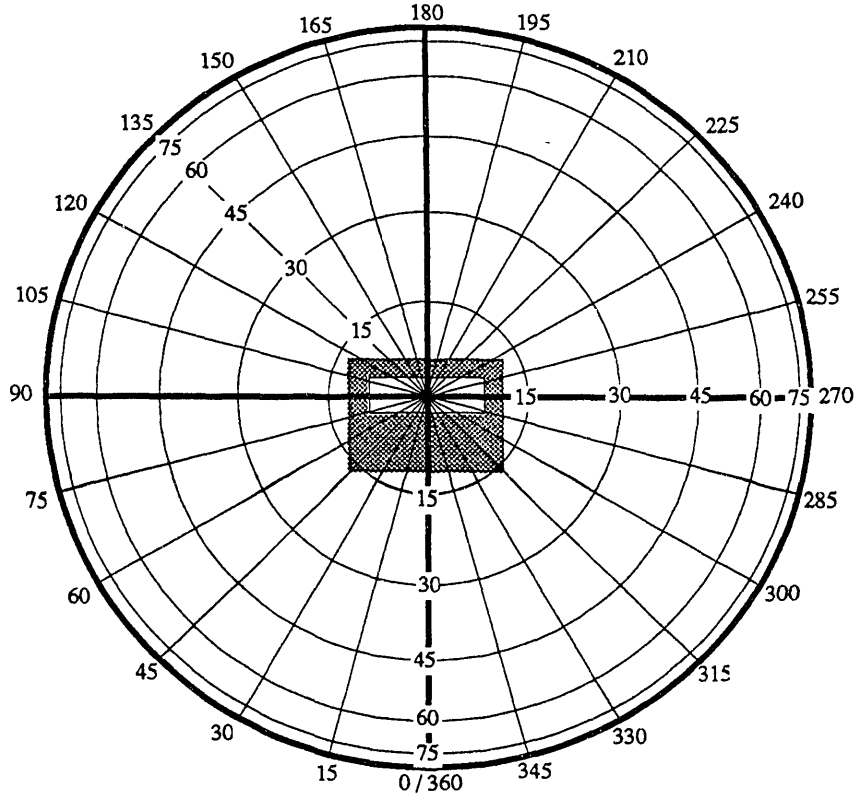

Figure 8.

Projection of the window-facing hemisphere, showing the incoming directions considered for the directional workplane illuminance measurements, in zeta (0°-360°), theta (0°-90°) coordinates.

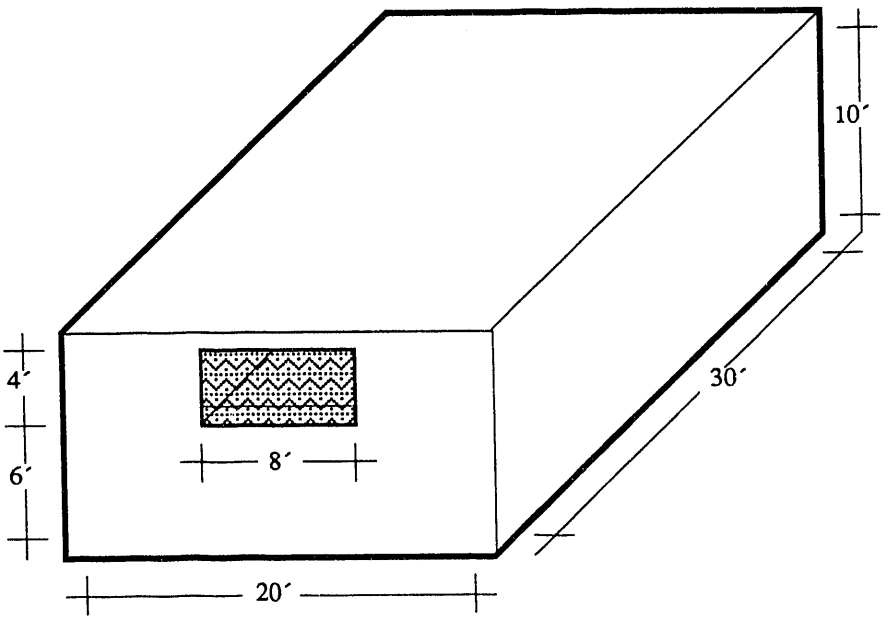

Figure 9.

The **4´x 8´** aperture considered for the **clear glass, BHDS and BHDS-2** measurements.

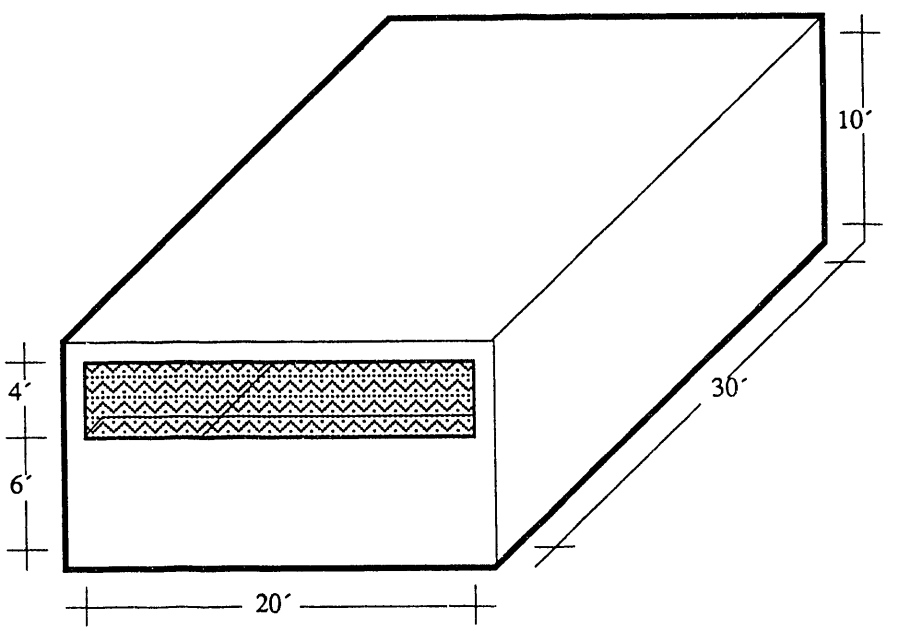

Figure 10.

The **4´x 20´** aperture considered for the **clear glass and BHDS** measurements.

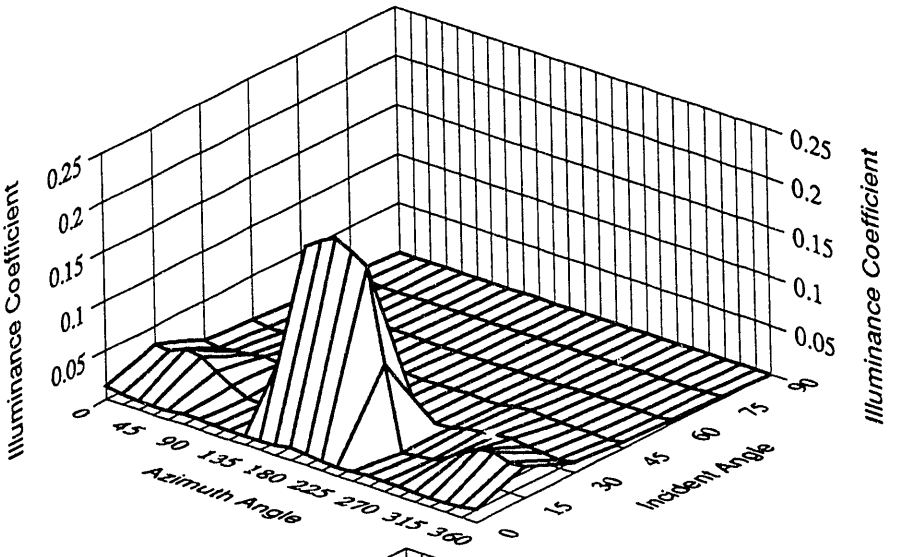

Figure 11.

Directional workplane illuminance coefficients for **4' x 8'** aperture of **clear glass** at **17.5'** from window wall.

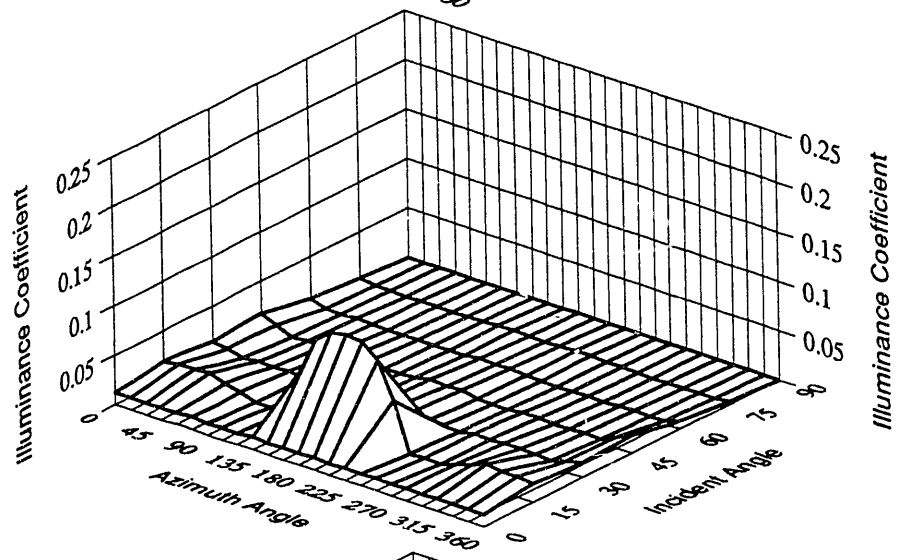

Figure 12.

Directional workplane illuminance coefficients for **4' x 8'** aperture of **BHDS** at **17.5'** from window wall.

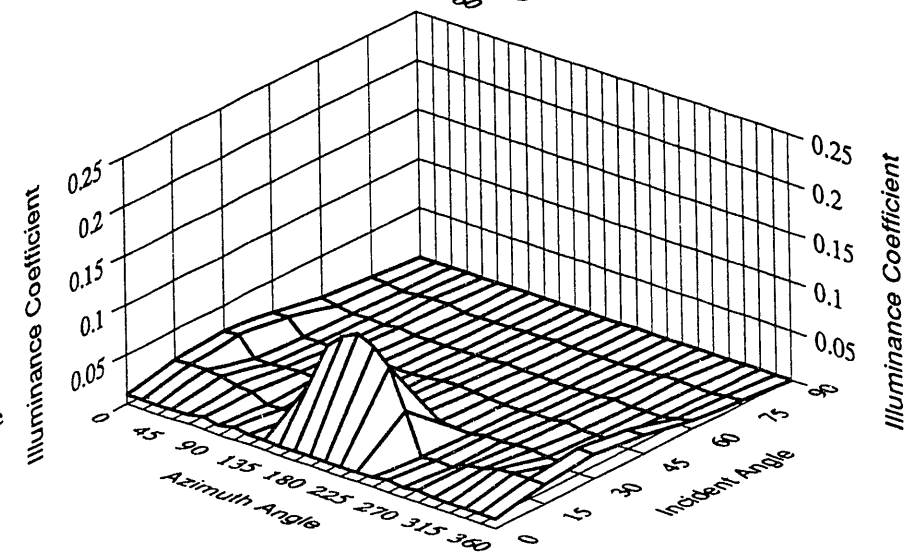

Figure 13.

Directional workplane illuminance coefficients for **4' x 8'** aperture of **BHDS-2** at **17.5'** from window wall.

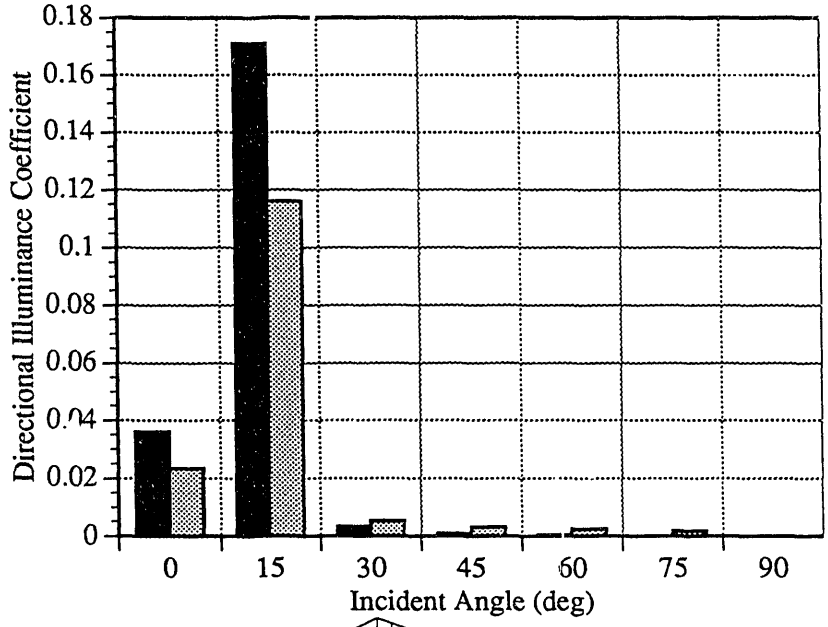

Figure 14.

Directional workplane illuminance coefficients for **4' x 20'** aperture of **clear glass** and **BHDS** at **27.5'** from window wall for incoming directions on a plane normal to the window (180° zeta angle).

clear glass

BHDS

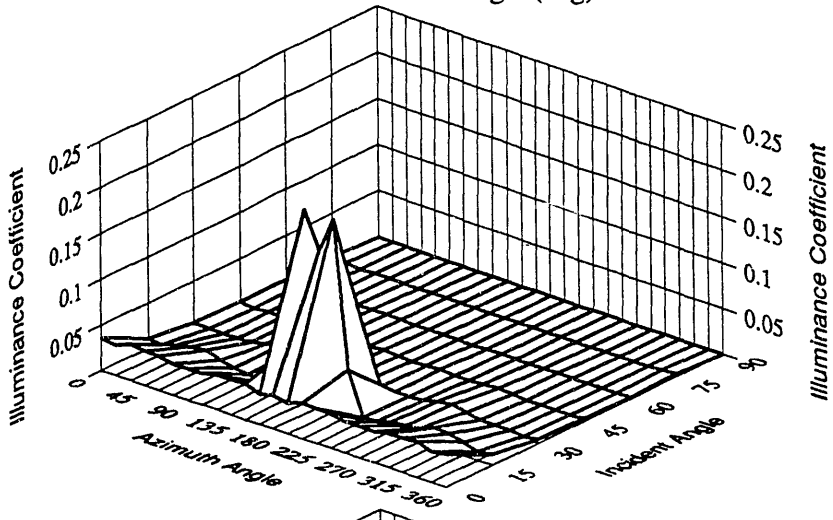

Figure 15.

Directional workplane illuminance coefficients for **4' x 20'** aperture of **clear glass** at **27.5'** from window wall.

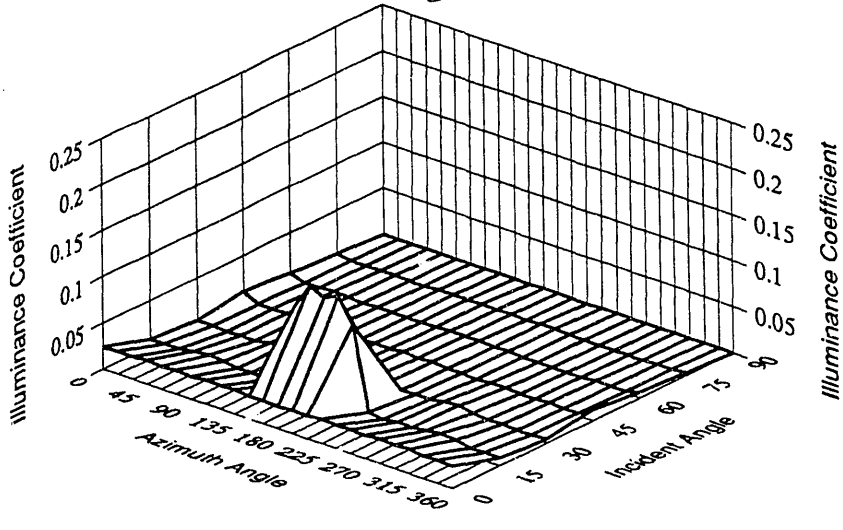

Figure 16.

Directional workplane illuminance coefficients for **4' x 20'** aperture of **BHDS** at **27.5'** from window wall.

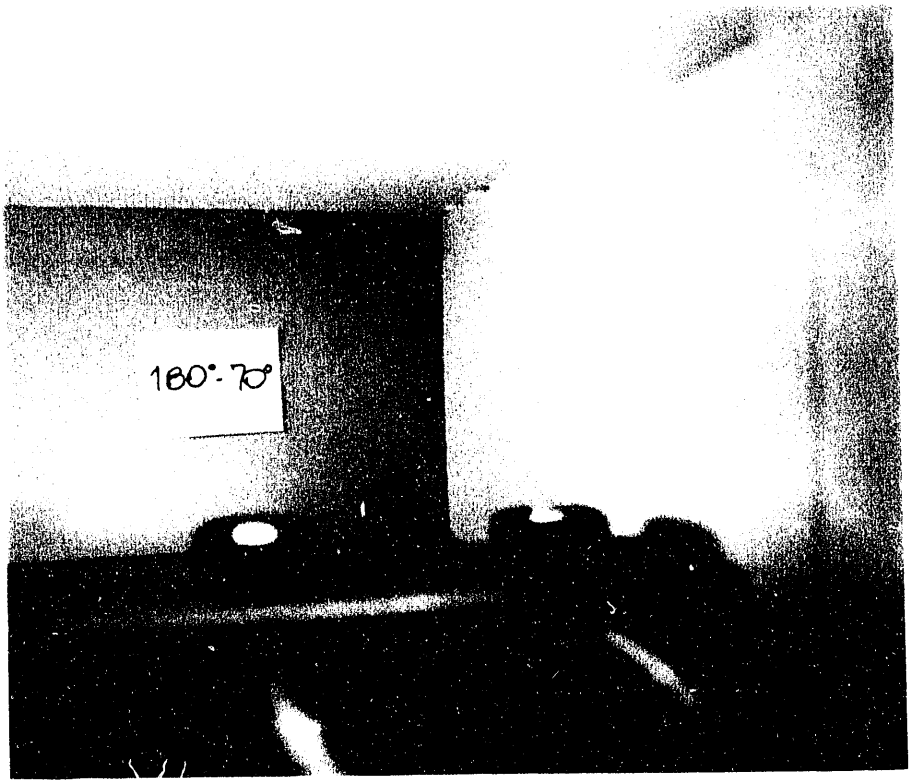

Figure 17.

Scale model photograph of the luminance distribution for the 4´x 8´ **HDS** aperture with sun at **180°** zeta and **70°** theta coordinates (see Figure 8).

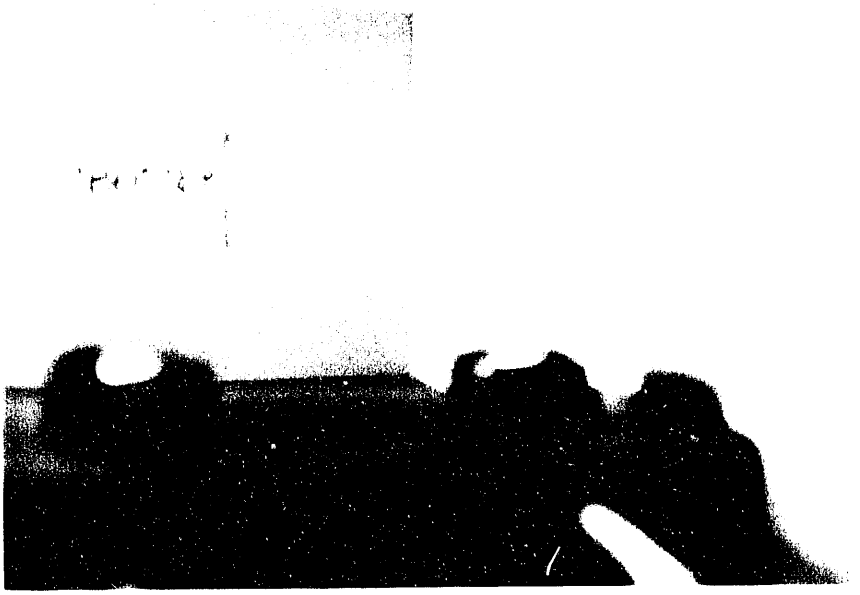

Figure 18.

Scale model photograph of the luminance distribution for the 4´x 8´ **BHDS** aperture with sun at **180°** zeta and **70°** theta coordinates (see Figure 8).

Figure 19.

Workplane illuminance distribution for the CIE **clear sky** through **South**-facing **4′x 8′** clear glass, BHDS and BHDS-2 apertures at **12:00 Noon** on **June 21** for the San Francisco climate.

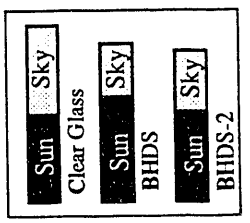

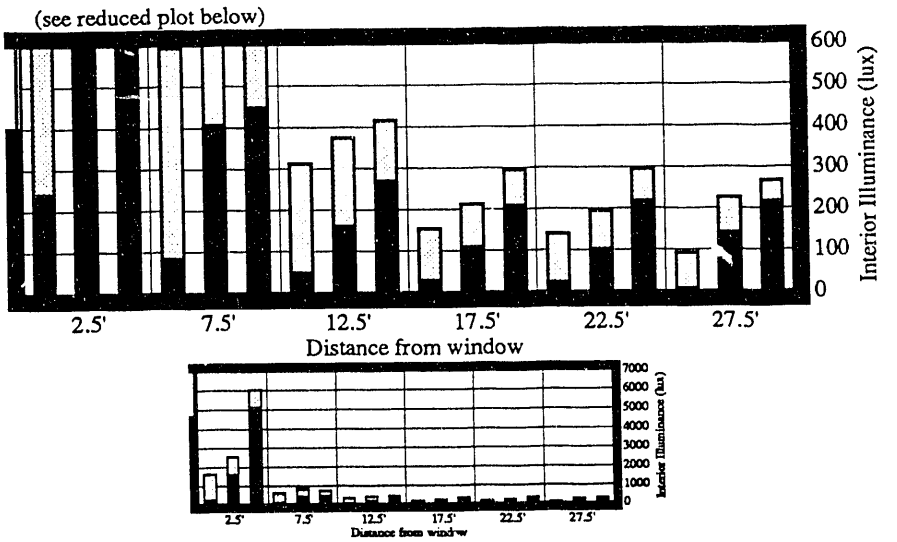

Figure 20.

Workplane illuminance distribution for the CIE **clear sky** through **South**-facing **4′x 8′** clear glass, BHDS and BHDS-2 apertures at **12:00 Noon** on **December 21** for the San Francisco climate.

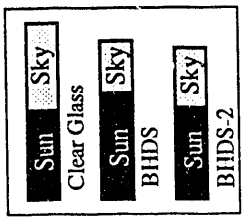

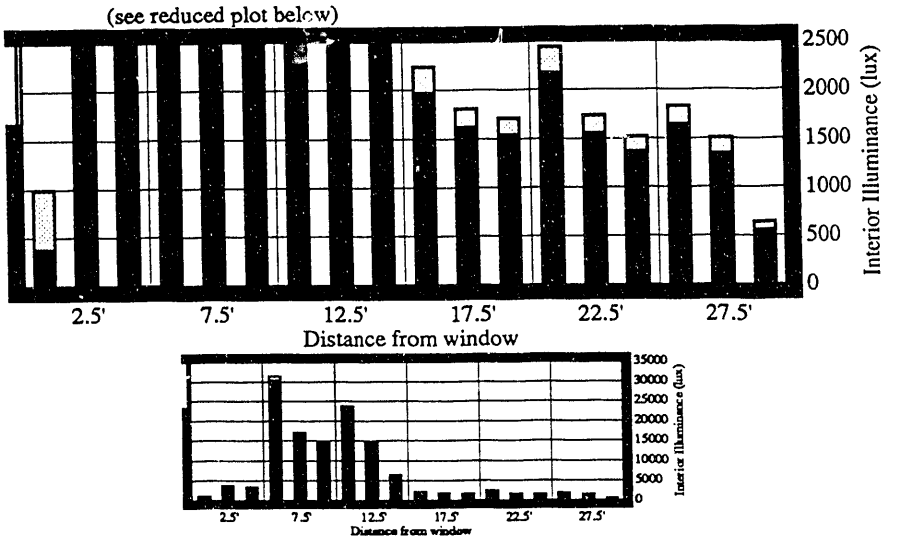

Figure 21.

Workplane illuminance distribution for the CIE **overcast sky** through **4′x 8′** clear glass, BHDS and BHDS-2 apertures at **12:00 Noon** on **June 21** for the San Francisco climate.

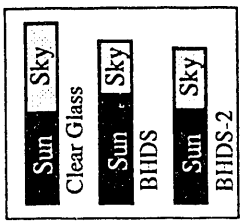

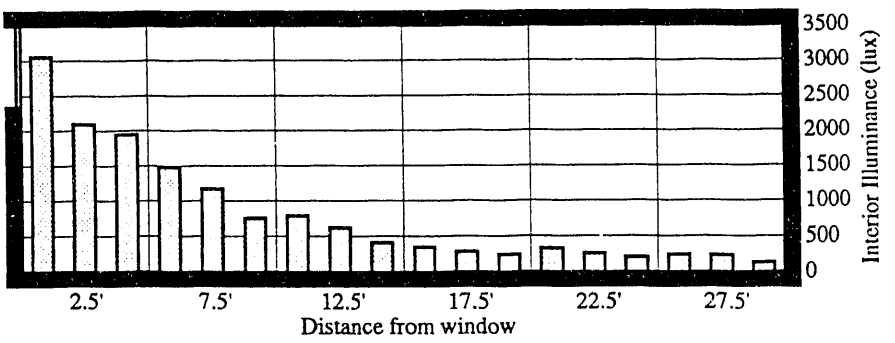

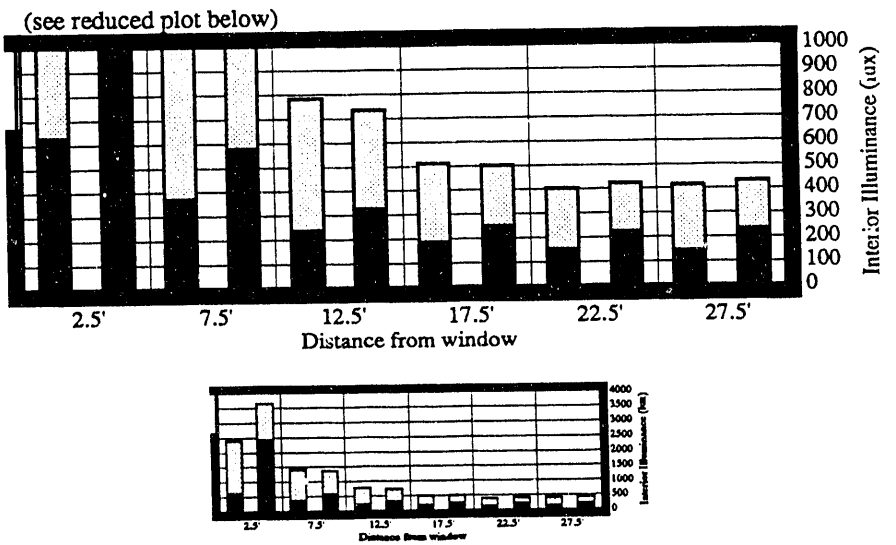

Figure 22.

Workplane illuminance distribution for the CIE **clear sky** through **South**-facing **4'x 20'** clear glass and BHDS apertures at **12:00 Noon** on **June 21** for the San Francisco climate.

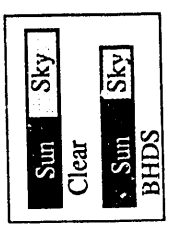

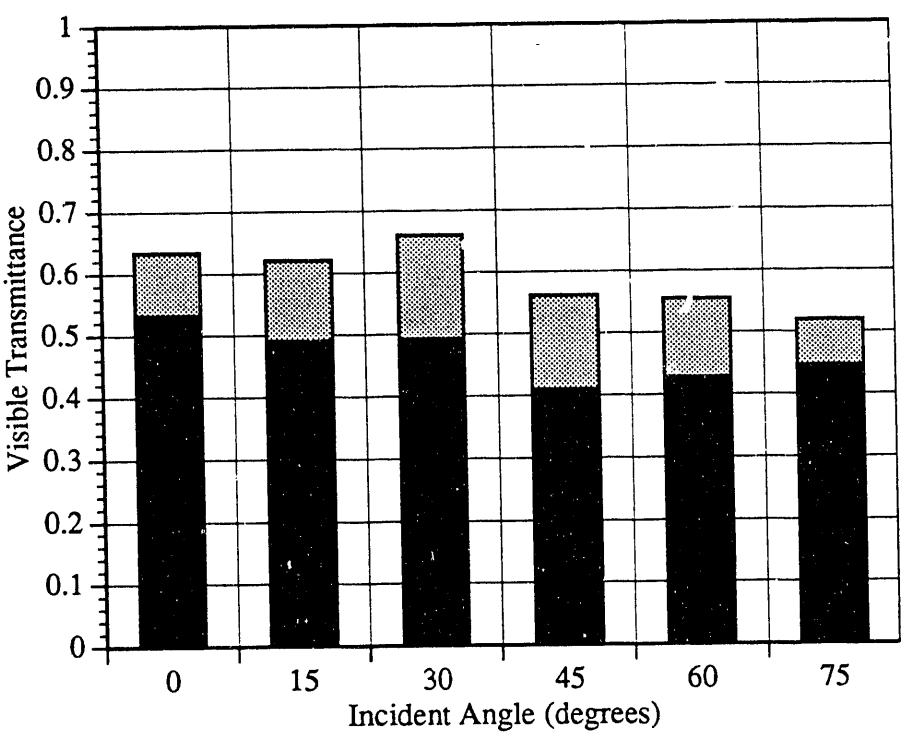

Figure 23.

The total, specular and diffracted transmittance of **BHDS** for the **visible** spectrum.

Diffracted

Specular

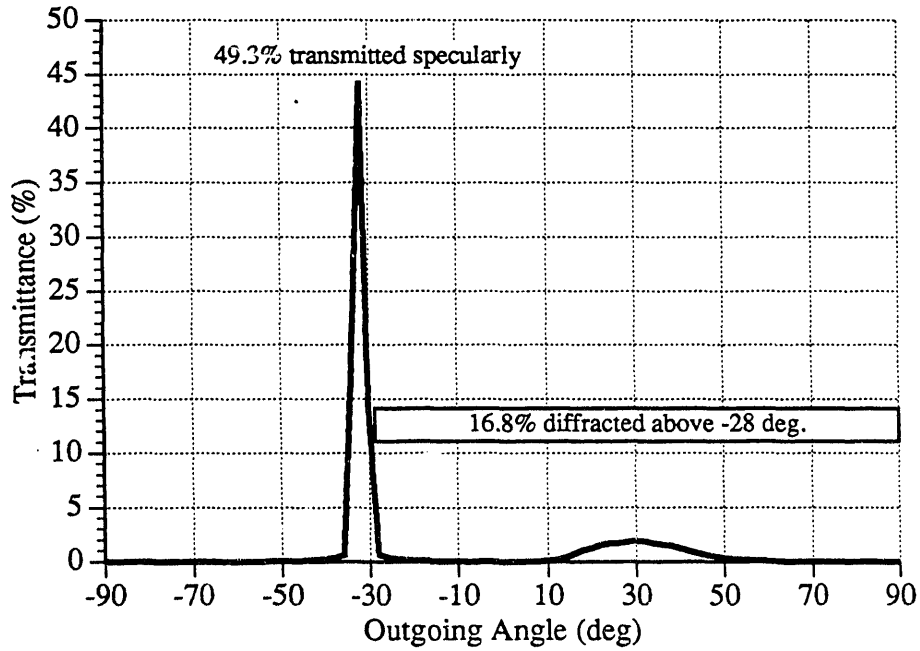

Figure 24.

The **bi-directional visible transmittance** of the **BHDS** for 30° incident angle of incoming radiation (maximum diffraction).

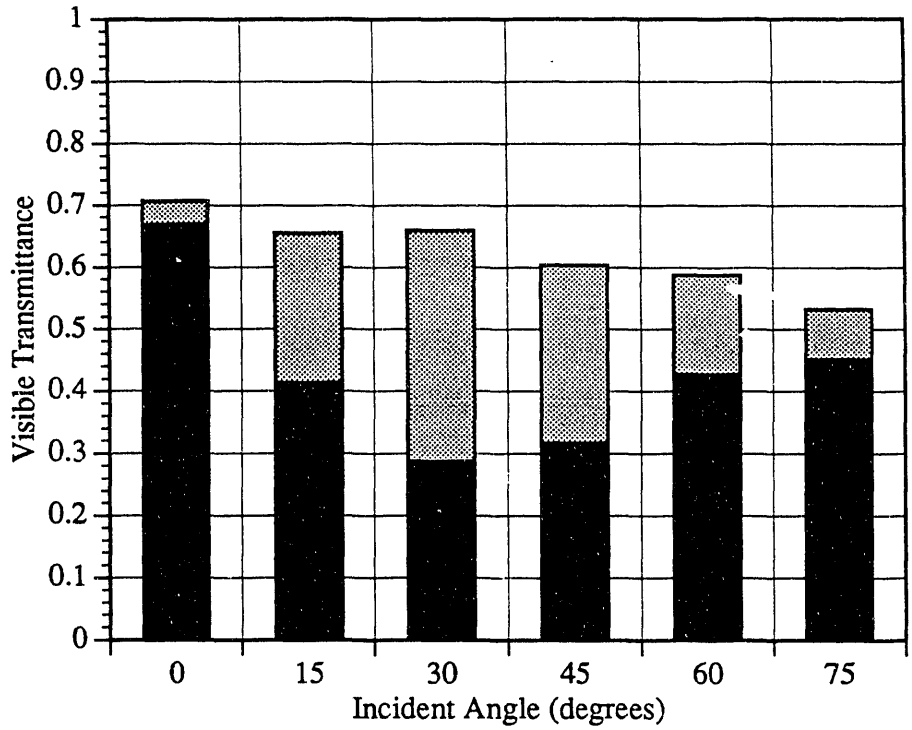

Figure 25.

The total, specular and diffracted transmittance of **HDS** for the **visible** spectrum.

Diffracted

Specular

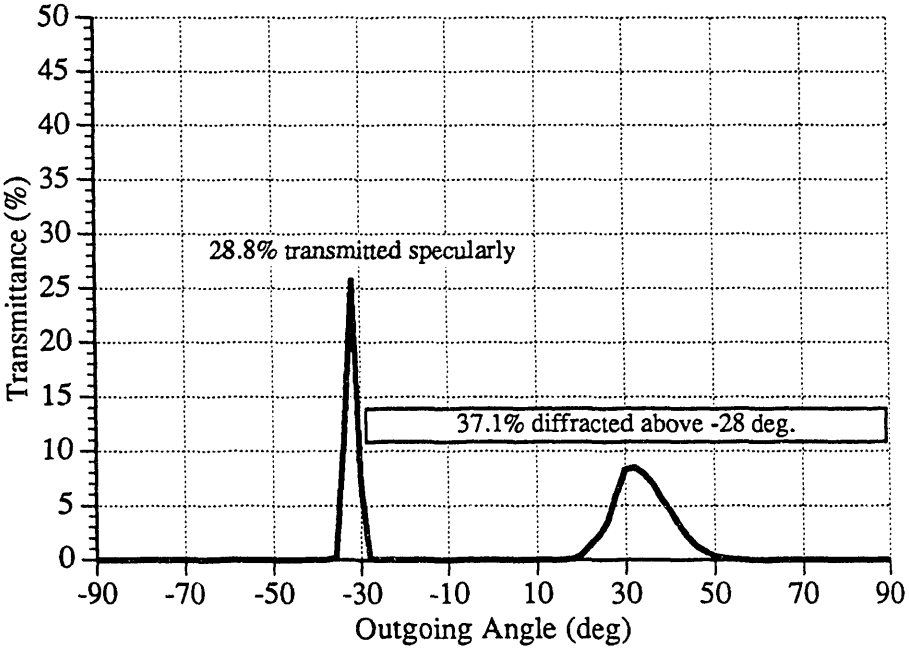

Figure 26.

The **bi-directional visible transmittance** of the **HDS** for **30°** incident angle of incoming radiation (maximum diffraction).

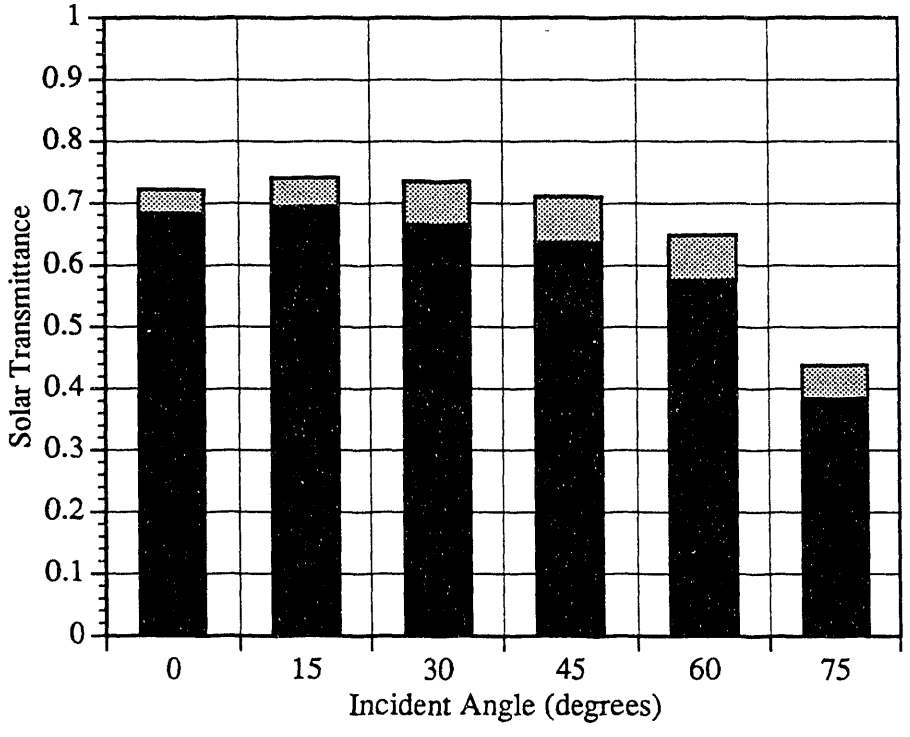

Figure 27.

The total **transmittance** of **BHDS** for the **total solar** spectrum.

Diffracted

Specular

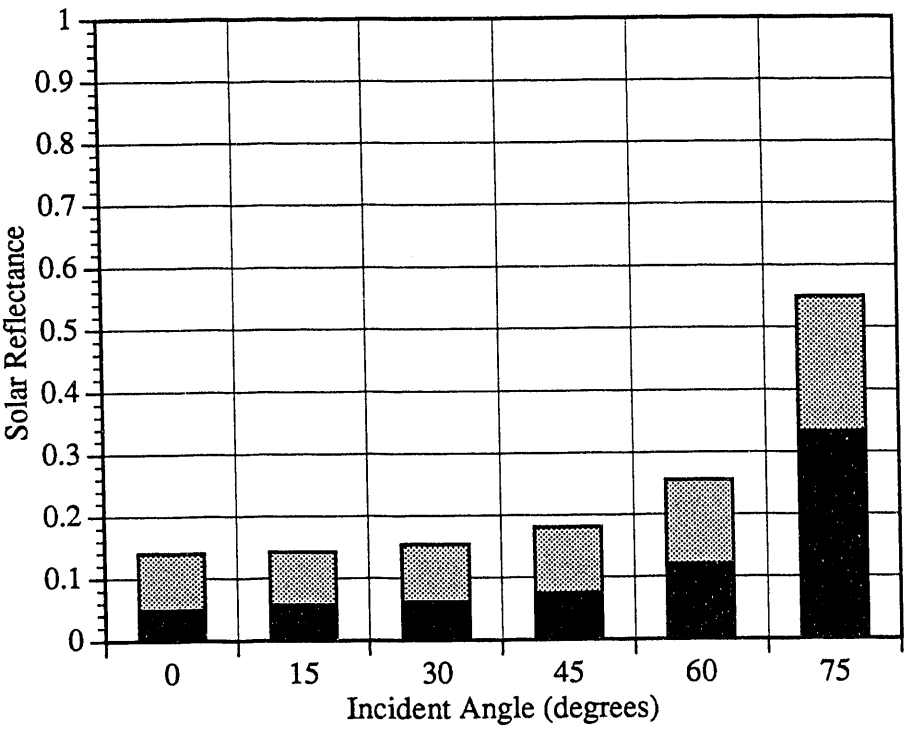

Figure 28.

The total **reflectance** of **BHDS** for the **total solar** spectrum.

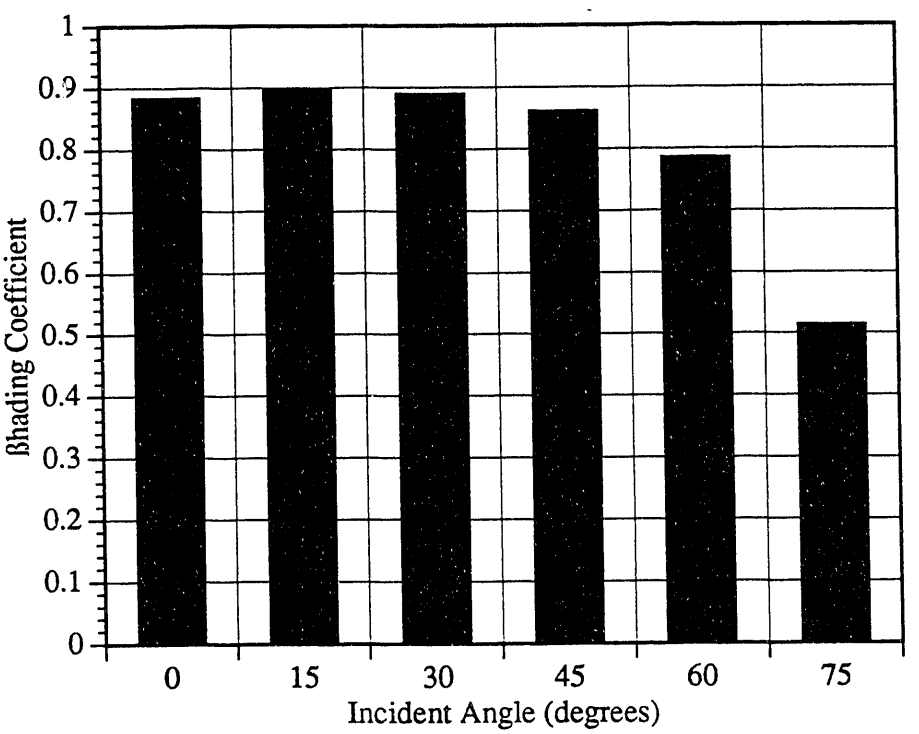

Figure 29.

The shading coefficient of the BHDS.

DATE
FILMED
11/5/93
END